Regular Article

PHYSICAL CHEMISTRY RESEARCH
Published by the
Iranian Chemical Society
www.physchemres.org
info@physchemres.org

Phys. Chem. Res., Vol. 9, No. 4, 591-603, December 2021
DOI: 10.22036/PCR.2021.282956.1911

Synthesis, PASS, *In Silico* ADMET and Thermodynamic Studies of Some Galactopyranoside Esters

U. Hanee[a], M.R. Rahman[b] and M.M. Matin[a,*]

[a]*Bioorganic and Medicinal Chemistry Laboratory, Department of Chemistry, Faculty of Science, University of Chittagong, Chittagong, 4331, Bangladesh*

[b]*Department of Chemical Engineering and Energy Sustainability, Faculty of Engineering, Universiti Malaysia Sarawak, Jalan Datuk Mohammad Musa, Kota Samarahan, 94300, Malaysia*

(Received 24 April 2021, Accepted 7 June 2021)

Due to their biodegradability and lower sideeffects, many sugar esters (SEs) have received much attention from researchers and been widely applied in medicinal chemistry. In this respect, methyl 6-*O*-pentanoyl-α-d-galactopyranoside, obtained from methyl α-d-galactopyranoside (MDG) using direct site-selective unimolar pentanoylation, was converted into four 2,3,4-tri-*O*-acyl esters in reasonably high yields. All the compounds were characterized by spectroscopic techniques. The results of Prediction of Activity Spectra for Substances (PASS) analysis indicated that the MDG esters had many potential biological activities. More specifically, the alkyl ester derivatives had higher antimicrobial potential than those of the sulfonyl ester. In addition, their absorption, distribution, metabolism, excretion and toxicity (ADMET) prediction revealed that most of the SEs had acceptable drug-related safety parameters. In this regard, the thermodynamic properties of galactopyranosides were also investigated and are reported herein.

Keywords: MEP, Methyl α-d-galactopyranoside esters, HOMO-LUMO, Sugar esters, Thermodynamic properties

INTRODUCTION

The unique and significant structural diversity of naturally occurring carbohydrates, especially those with monosaccharide structures, makes them the best recognition markers for numerous physiological activities [1-3]. Carbohydrates are found to have much higher structural diversity than proteins and lipids, and this might be related to their specific cellular action. Among the carbohydrates, galactose (Gal), a C-4 epimer of glucose, has been widely used to build up biologically active glycoconjugates in living organisms [4]. In addition to its dietary and metabolic functions, Gal has multiple clinical applications [5-7].

For instance, Gal was found to act as an important component of binding sites for a wide range of pathogens, selectins, and toxins [8-9]. Furthermore, its disaccharide Galα1-4Gal is considered to be the most powerful binding adhesin of *Streptococcus suis* involved in *S. suis* interactions with host cells. Hence, Gal residue is associated with diverse pathologic conditions and mimicking of the evolution of pathogen-binding protein isoforms [10-12]. Despite the above-mentioned useful functions and applications of Gal, extensive research has been performed to modify its various stereocenters to minimize the immunogenic effects of galactose-carrying biotherapeutic products [13-15].

Several studies have shown that galactose residues are the key molecules for targeting hepatocytes involved in tumor cells [16]. In this regard, Liu *et al.* [17] successfully synthesized butyryl galactose ester (But-Gal) and found that galactose ester-modified microemulsions could be used as nanocarriers for the therapy of hepatoma. The modification of monosaccharide sugars with an ester group or multiple ester groups), hence called sugar esters (SEs), extended

*Corresponding author. E-mail: mahbubchem@cu.ac.bd

their application to a wider range of products, including low-calorie sweeteners, flavorings and biosurfactants/ emulsifiers in foods, food additives, detergents and pharmaceutical, biomedical, cosmetic products [18-21]. In addition, SEs have been suggested to have potential activity against SARS-CoV-2 main protease [22]. Furthermore, acyl galactopyranosides, such as 5-aminosalicylic acid ester, were found to be highly active not only in the treatment of inflammatory bowel disease (IBD) but also against *Staphylococcus aureus* and *Escherichia coli* [23-24].

However, monosaccharides, compared to other biomolecules such as amino acids and nucleosides, pose more unique synthetic challenges [25]. The key issue is that each sugar monomer contains several hydroxyl (OH) groups, each representing a potential site of chemical reactivity [26-28]; thus, in most cases, a mixture of mono-, di- and polyesters is formed [29-31]. Many methods, such as (i) direct [32-33], (ii) catalytic [34-35], (iii) protection-deprotection [36-38], (iv) enzymatic [39] and (iv) microwave [40] methods, have been developed and employed for organic synthesis [28,31]. Different methods gave different selectivity and product yield [31]. In the present study, we employed the direct acylation method, while maintaining some conditions, to achieve site-selective 6-*O*-pentanoylgalactopyranoside [41].

Although a plethora of studies have examined the role of Gal sugar in human health and diseases, many of its functions still remain unknown due to its biological diversity. Furthermore, more studies are needed to clarify the biological significance of anti-Gal antibodies and the stereoelectronic effects of galactosylation, sialylation, and acylation in different biological activities of the body [42]. Accordingly, we endeavored to synthesize and explore the use of different SEs [43]. Herein, we report on the synthesis of some 6-*O*-pentanoyl-α-d-galactopyranoside esters using PASS (Prediction of Activity Spectra for Substances) prediction and *in silico* ADMET (absorption, distribution, metabolism, excretion, and toxicity) and thermodynamic properties.

EXPERIMENTAL

General Methods

The necessary reagent grade chemicals and solvents are commercially available. Some solvents, such as *n*-hexane, ethyl acetate, *etc*., were distilled before use. The solvent system(s) used for thin-layer chromatography (TLC) and column chromatography (CC) included different proportions of chloroform/methanol and/or *n*-hexane/ethyl acetate. Silica gel plates (Kieselgel 60 F 254) were used for TLC. The spots were visualized by spraying the plates with 1% H_2SO_4 in methanol, followed by heating the plates at +150 °C until coloration appeared. The compounds were purified by CC using silica gel G60. The solutions were concentrated under reduced pressure below 40 °C in a rotary evaporator (Büchi R-100, Switzerland). FT-IR spectra were recorded on KBr discs. Melting points were uncorrected. The compounds were characterized by ^{1}H (400 MHz) and ^{13}C (100 MHz) NMR spectra, which were recorded in $CDCl_3$ solution. Chemical shifts were reported in δ units (ppm) with reference to TMS as an internal standard. Coupling constants values are reported in Hertz (Hz).

Synthesis

Methyl-6-*O*-pentanoyl-α-d-galactopyranoside (2). The regioselective methyl 6-*O*-pentanoyl-α-d-galactopyranoside was prepared according to a literature procedure from methyl α-d-galactopyranoside (MDG, 1) in 49% yield as a brownish solid (m.p.: 95-96 °C) [41].

General procedure for 2,3,4-tri-*O*-acylation of compound 2. Acyl halide (MsCl/TsCl/*iso*-PentCl/BzCl, 3.3 eq) was added slowly to a solution of triol 2 (0.1 g) in pyridine (1 ml) at 0 ºC, followed by addition of a catalytic amount of DMAP. The reaction mixture was allowed to attain room temperature, and stirring was continued for 10-12 h. The reaction mixture was quenched with ice water and extracted with DCM (3 × 3 ml). The DCM layer was washed successively with 5% hydrochloric acid, saturated aqueous sodium hydrogen carbonate solution, and brine. Then, the DCM layer was dried and concentrated. Column chromatography (CC) of the obtained residue with *n*-hexane/ethyl acetate as an eluent furnished the corresponding 2,3,4-tri-*O*-acyl products (3-6) in good yields.

Methyl-2,3,4-tri-*O*-mesyl-6-*O*-pentanoyl-α-d-galactopyranoside (3). Thick syrup; yield: 94%; R_f = 0.54 (*n*-hexane/EA = 4/1); FT-IR (KBr): 1738 (CO), 1364, 1362, 1354 (SO_2), 1072 cm^{-1} (pyranose ring); ^{1}H NMR (400 MHz,

$CDCl_3$): δ_H 4.98 (dd, J = 10.2 and 3.4 Hz, 1H, H-3), 4.85-4.89 (m, 2H, H-1 and H-4), 4.78 (dd, J = 10.0 and 3.6 Hz, 1H, H-2), 4.34-4.39 (m, 2H, H-6 and H-6′), 3.98-4.01 (m, 1H, H-5), 3.38 (s, 3H, OCH_3), 3.35 (s, 3H, SO_2CH_3), 3.33 (s, 3H, SO_2CH_3), 3.24 (s, 3H, SO_2CH_3), 2.33 [t, J = 7.6 Hz, 2H, $CH_3(CH_2)_2CH_2CO$], 1.60-1.67 (m, 2H, $CH_3CH_2CH_2CH_2CO$), 1.26-1.36 [m, 2H, $CH_3CH_2(CH_2)_2CO$], 0.91 [t, 3H, J = 7.0 Hz, $CH_3(CH_2)_3CO$].

Methyl-6-*O*-pentanoyl-2,3,4-tri-*O*-tosyl-α-d-galactopyranoside (4). Clear syrup; yield: 76%; R_f = 0.59 (*n*-hexane/EA = 4/1); FT-IR (KBr): 1743 (CO), 1369, 1365, 1362 (SO_2), 1055 cm^{-1} (pyranose ring); ^{1}H NMR (400 MHz, $CDCl_3$): δ_H 7.81 (d, J = 7.6 Hz, 2H, Ar-*H*), 7.76 (d, J = 8.4 Hz, 2H, Ar-*H*), 7.61 (d, J = 8.4 Hz, 2H, Ar-*H*), 7.37 (t, J = 8.4 Hz, 4H, Ar-*H*), 7.26 (d, J = 8.0 Hz, 2H, Ar-*H*), 4.88 (dd, J = 9.8 and 3.2 Hz, 1H, H-3), 4.81-4.85 (m, 2H, H-1 and H-4), 4.73 (dd, J = 10.0 and 3.6 Hz, 1H, H-2), 4.16-4.33 (m, 2H, H-6 and H-6′), 3.98-4.01 (m, 1H, H-5), 3.38 (s, 3H, OCH_3), 2.49 (s, 3H, $CH_3C_6H_4SO_2$), 2.48 (s, 3H, $CH_3C_6H_4SO_2$), 2.45 (s, 3H, $CH_3C_6H_4SO_2$), 2.34 [t, J = 7.6 Hz, 2H, $CH_3(CH_2)_2CH_2CO$], 158-1.67 (m, 2H, $CH_3CH_2CH_2CH_2CO$), 1.29-1.39 (m, 2H, $CH_3CH_2(CH_2)_2CO$], 0.93 [t, J = 7.6 Hz, 3H, $CH_3(CH_2)_3CO$]; ^{13}C NMR (100 MHz, $CDCl_3$): δ_C 173.5 [$CH_3(CH_2)_3CO$], 145.4, 145.1(2), 133.6, 133.0, 132.8, 129.9(2), 129.7, 128.0(2), 128.0 (Ar-*C*), 97.7 (C-1), 73.6, 69.0, 68.4 (C-2/C-3/C-5), 67.2 (C-4), 62.4 (C-6), 55.6 (OCH_3), 33.8 [$CH_3(CH_2)_2CH_2CO$], 26.9 ($CH_3CH_2CH_2CH_2CO$), 22.7 [$CH_3CH_2(CH_2)_2CO$], 21.7(2), 21.6 (3×$CH_3C_6H_4CO$), 13.6 [$CH_3(CH_2)_3CO$].

Methyl-2,3,4-tri-*O*-isopentanoyl-6-*O*-pentanoyl-α-d-galactopyranoside (5). Syrup; yield: 87%; R_f = 0.52 (*n*-hexane/EA = 4/1); FT-IR (KBr): 1739, 1733, 1722, 1719 (CO), 1066 cm^{-1} (pyranose ring); ^{1}H NMR (400 MHz, $CDCl_3$): δ_H 5.47 (d, J = 3.2 Hz, 1H, H-4), 5.42 (dd, J = 10.8 and 3.2 Hz, 1H, H-3), 5.17 (dd, J = 10.8 and 3.6 Hz, 1H, H-2), 5.00 (d, J = 3.4 Hz, 1H, H-1), 4.16-4.20 (m, 1H, H-5), 4.08-4.13 (m, 2H, H-6 and H-6′), 3.41 (s, 3H, OCH_3), 2.37 [t, J = 7.6 Hz, 2H, $CH_3(CH_2)_2CH_2CO$], 2.25-2.31 [m, 6H, 3×$(CH_3)_2CHCH_2CO$], 2.08-2.14 [m, 3H, 3×$(CH_3)_2CHCH_2CO$], 1.58-1.65 (m, 2H, $CH_3CH_2CH_2CH_2CO$), 1.27-1.37 [m, 2H, $CH_3CH_2(CH_2)_2CO$], 0.98(2), 0.97 [3×s, 3×6H, 3×$(CH_3)_2CHCH_2CO$], 0.92 [t, J = 7.2 Hz, 3H, $CH_3(CH_2)_3CO$].

Methyl-2,3,4-tri-*O*-benzoyl-6-*O*-pentanoyl-α-d-galactopyranoside (6). Oil; yield: 72%; R_f = 0.64 (*n*-hexane/EA = 4/1); FT-IR (KBr): 1745, 1743, 1740, 1738 (CO), 1054 cm^{-1} (pyranose ring); ^{1}H NMR (400 MHz, $CDCl_3$): δ_H 8.13 (d, J = 7.4 Hz, 2H, Ar-*H*), 7.99-8.09 (m, 4H, Ar-*H*), 7.58-7.66 (m, 2H, Ar-*H*), 7.43-7.56 (m, 5H, Ar-*H*), 7.35-7.42 (m, 2H, Ar-*H*), 5.74 (dd, J = 10.4 and 2.8 Hz, H 1H, -3), 5.68 (dd, J = 10.4 and 3.2 Hz, 1H, H-2), 5.67 (t, J = 3.2 Hz, 1H, H-4), 5.21 (d, J = 3.2 Hz, 1H, H-1), 4.58 (dd, J = 11.2 and 5.6 Hz, 1H, H-6), 4.45 (dd, J = 11.2 and 6.8 Hz, 1H, H-6′), 4.20-4.24 (m, 1H, H-5), 3.46 (s, 3H, OCH_3), 2.38 [t, J = 7.4 Hz, 2H, $CH_3(CH_2)_2CH_2CO$], 160-1.69 (m, 2H, $CH_3CH_2CH_2CH_2CO$), 1.33-1.41 (m, 2H, $CH_3CH_2(CH_2)_2CO$], 0.94 [t, J = 7.4 Hz, 3H, $CH_3(CH_2)_3CO$]; ^{13}C NMR (100 MHz, $CDCl_3$): δ_C 173.7 [$CH_3(CH_2)_3CO$], 166.1, 165.8, 165.6 (C_6H_5CO), 133.7, 133.4, 133.2, 130.2 (3), 129.8(2), 129.7, 128.5(2), 128.4 (Ar-*C*), 97.6 (C-1), 70.8, 68.9, 68.2 (C-2/C-3/C-5), 67.6 (C-4), 62.7 (C-6), 55.5 (OCH_3), 33.9 [$CH_3(CH_2)_2CH_2CO$], 27.0 ($CH_3CH_2CH_2CH_2CO$), 22.2 [$CH_3CH_2(CH_2)_2CO$], 13.6 [$CH_3(CH_2)_3CO$].

PASS Prediction

PASS is a software product designed for the prediction of a wide range of biological activities [43]. PASS can predict various biological activities with 90% accuracy. Initially, all the structures of galactopyranosides were drawn using ChemDraw 16.0 with the appropriate geometry; then, they were converted into SD format. Finally, they were used to predict the biological activity spectrum using PASS online software (http://www.pharmaexpert.ru/PASSonline/index.php) [44]. The predicted results were designated as Pa (probability for active compound) and Pi (probability for inactive compound), where Pa > Pi and their values varied from 0.000 to 1.000 (Pa + Pi ≠ 1).

ADME/T and Drug Friendliness Analysis

The ADMET and pharmacokinetic properties of the SEs 2-6 were predicted *in silico* using the pkCSM online server [45]. Generally, *in silico* ADMET predictions are preferred since rapid ADMET evaluation can minimize serious failures in different stages of *in vivo* drug discovery. For ADMET prediction, first, the structures of all compounds (1-6) were drawn by ChemDraw 18.0 with

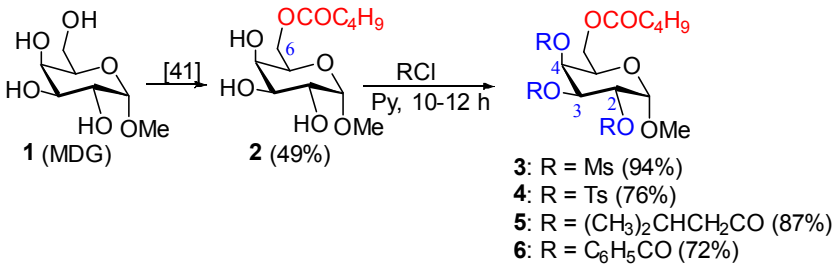

Scheme 1. Synthesis of galactopyranoside esters 3-6

the appropriate geometry; then, they were converted to the InChIkey, SMILES and SD formats to be used as input for different analyses. Finally, these file formats were used to predict the ADMET properties using the pkCSM-pharmacokinetics online server (http://biosig.unimelb.edu.au) [45].

DFT Optimization and Thermodynamic Calculations

The accurate prediction of the structure and energetics, along with the molecular orbitals, is crucial for the understanding and characterization of various properties of carbohydrate molecules. In the past few decades, density functional theory (DFT)-based quantum mechanical methods have been widely used to predict thermal, molecular orbital (MO), and molecular electrostatic potential (MEP) properties [46]. To predict thermodynamic and MO properties, the initial geometry of MDG (1) was obtained from the ChemSpider database. Then, all other structures (2-6) were drawn using the GaussView (5.0) program [47] while maintaining proper stereochemistry. At this stage, all the compounds were optimized at DFT B3LYP/6-31G(d,p) basis set at 298.1 K and 1.0 atm without any solvent on a computer with an Intel Core i7 computer. These optimized structures were used for various thermodynamic calculations. In addition, WebMO server and GaussSum 3.0 software were used in this study.

RESULTS AND DISCUSSION

2,3,4-Tri-*O*-acyl Esters of 6-*O*-Pentanoylgalactopyranoside 2

Initially, site-selective 6-*O*-pentanoyl MDG (2) was prepared according to a procedure from MDG (1) in 49% yield as a brownish solid (m.p.: 95-96 °C) [41]. Once the MDG (2) was prepared, its 2,3,4-tri-*O*-acylation was carried out with four acylating agents. Thus, treatment of triol 2 with trimolar mesyl chloride and purification resulted in a faster-moving syrup (94%, Scheme 1). Its FT-IR spectrum showed three SO_2 stretching bands as well as a carbonyl band, indicating the attachment of three mesyl groups in the molecule. This was further confirmed by the appearance of three three-proton singlets at δ 3.35, 3.33 and 3.24. Also, a three-proton singlet at δ 3.38 was attributed to the galactosidic OCH_3 group. Significant downfield shifts were observed for H-2 (δ 4.78), H-3 (δ 4.98), and H-4 (δ 4.85-4.89) compared to that of their precursor 2 [41], indicating the attachment of mesyl groups at C-2, C-3 and C-4 positions of the molecule. A detailed analysis of the spectrum enabled us to assign its structure as methyl-2,3,4-tri-*O*-mesyl-6-*O*-pentanoyl-α-d-galactopyranoside (3).

Similarly, the tri-*O*-tosylation of pentanoate 2 in dry pyridine for 12 h gave a clear syrupy compound in good yield (Scheme 1). Its FT-IR spectrum showed a carbonyl stretching band at 1743 cm^{-1} and sulfonyl stretching bands at 1369, 1365 and 1362 cm^{-1}. Furthermore, its ^{1}H NMR spectrum showed the presence of twelve aromatic protons at δ 7.81 (2H), 7.76 (2H), 7.61 (2H), 7.37 (4H) and 7.26 (2H) and three three-proton singlets at δ 2.49, 2.48 and 2.45, indicating the attachment of three tosyl groups in the molecule. This was further supported by the analysis of its ^{13}C NMR spectrum, which revealed the presence of carbon signals at δ 145.4, 145.1 (2), 133.6, 133.0, 132.8, 129.9 (2), 129.7, 128.0 (2), 128.0, 21.7 (2) and 21.6. Thus, the structure of the compound was assigned as methyl 6-*O*-pentanoyl-2,3,4-tri-*O*-tosyl-α-d-galactopyranoside (4).

Table 1. PASS-predicted Biological Activities of Galactopyranosides 1-6

Drug	Biological activity							
	Antibacterial		Antifungal		Anticarcinogenic		Antioxidant	
	Pa	Pi	Pa	Pi	Pa	Pi	Pa	Pi
1	0.541	0.013	0.628	0.016	0.731	0.008	0.667	0.004
2	0.528	0.014	0.669	0.012	0.769	0.006	0.530	0.005
3	0.408	0.028	0.436	0.042	0.433	0.026	0.288	0.025
4	0.362	0.040	0.388	0.052	0.299	0.058	0.263	0.032
5	0.566	0.011	0.689	0.010	0.555	0.015	0.408	0.011
6	0.505	0.016	0.642	0.014	0.632	0.011	0.413	0.011
TTC	0.694	0.005	0.523	0.023	-	-	-	-
FCZ	-	-	0.726	0.008	-	-	-	-

Pa = probability 'to be active'; Pi = probability 'to be inactive'; TTC = tetracycline; FCZ = fluconazole.

In the next step, isopentanoyl chloride was used as a potential acylating agent, and a syrup was obtained in 87% yield (Scheme 1). The presence of four carbonyl bands at 1739, 1733, 1722 and 1719 cm^{-1} in its FT-IR spectrum indicated the attachment of three isopentanoyl groups in the molecule. Again, the presence of additional twenty-seven protons in its ^{1}H NMR, compared to the number of protons in its precursor 2, supported the above observation. Also, the signals of H-2, H-3 and H-4 were shifted downfield compared to that of their precursor compound 2 [41]. A detailed analysis of its spectral data established its structure as methyl-2,3,4-tri-*O*-isopentanoyl-6-*O*-pentanoyl-α-d-galactopyranoside (5).

Finally, the treatment of 6-*O*-pentanoate 2 with trimolar benzoyl chloride in dry pyridine gave an oil in good yield (Scheme 1). In its FT-IR spectrum, the compound showed characteristic stretching bands at 1745, 1743, 1740 and 1738 cm^{-1}. Its ^{1}H NMR spectrum showed additional fifteen aromatic protons at δ 8.13 (d, 2H), 7.99-8.09 (m, 4H), 7.58-7.66 (m, 2H), 7.43-7.56 (m, 5H), and 7.35-7.42 (m, 2H), indicating the attachment of three benzoyl groups in the molecule. Their corresponding carbon signals were also observed in its ^{13}C NMR spectrum. All these observations and analogy with compounds 3-5 confirmed its structure as methyl-2,3,4-tri-*O*-benzoyl-6-*O*-pentanoyl-α-d-galactopyranoside (6).

PASS-predicted Biological Activities

After the successful synthesis of galactopyranoside esters 2-6, the biological activities of these compounds were predicted using PASS online software (http://www.way2drug.com/passonline/) [43-44]. Although these compounds showed a plethora of biological activities, only their antibacterial, antifungal, anticarcinogenic, and antioxidant properties are presented in Table 1. For comparison, similar biological activities were predicted for tetracycline, a standard antibiotic, and fluconazole, a standard antifungal agent.

As Table 1 shows, while the incorporation of the pentanoyl group in MDM (1) increased its antifungal and anticarcinogenic properties, it decreased its antibacterial and antioxidant properties. Furthermore, the addition of both mesyl (3) and tosyl (4) groups decreased its antibacterial, antifungal, anticarcinogenic and antioxidant properties. However, the addition of isopentanoyl group, as in 5, increased both its antibacterial and antifungal properties, even more significantly than did the addition of monopentanoate 2. Overall, the alkyl ester groups (2, 5-6) had higher antimicrobial potential than did the sulphonyl ester groups (3-4) (Table 1).

ADMET Properties

The web-based rapid ADMET virtual screening or

Table 2. ADMET Calculation of Galactopyranoside-derived SEs 2-6

Drug	Absorption			Distribution		Metabolism	Excretion	Toxicity	
	C2P	HIA (%)	P-gpI	BBB (Permeability)	CNS (Permeability)	CYP3A4 substrate	Total clearance	hERG inhibitor	Toxicity (LD_{50})
1	-0.247	33.43	No	-0.992	-3.622	No	0.671	No	1.157
2	-0.141	61.53	No	-1.076	-3.237	No	1.557	No	1.620
3	0.107	100	Yes	-2.807	-3.517	No	1.701	No	2.373
4	-0.151	100	Yes	-2.864	-3.981	Yes	0.626	No	2.557
5	0.966	93.98	Yes	-1.675	-2.772	Yes	1.085	No	2.152
6	0.862	100	Yes	-1.608	-3.419	Yes	0.919	No	2.758
FZ	1.191	87.82	No	-1.200	-3.221	No	0.386	No	2.210

C2P = Caco-2 permeability (log Papp in 10^{-6} cm s^{-1}, >0.90 indicates high permeability); HIA = human intestinal absorption (%absorbed, >30% is better absorbed); P-gpI = P-glycoprotein inhibitor; BBB (blood-brain barrier) is expressed as logBB (logBB > -1.0 is moderately cross blood-brain barrier); CNS is expressed as logPS (logPS > -2.0 can easily penetrate the CNS); Total clearance is expressed in log ml min^{-1} kg^{-1}; Toxicity is calculated in oral rat acute toxicity (mol/kg); FZ = fluconazole.

filtering and prioritization of chemical structures can help researchers to identify promising drug candidates [45,48]. Also, nowadays, comprehensive studies of ADMET properties are routinely carried out at the early stage of drug discovery to reduce the attrition rate [48]. In the present study, the ADMET properties of galactopyranosides 1-6 were predicted using the pkCSM online server (http://biosig.unimelb.edu.au) [45]. The results are shown in Table 2.

Caco-2 permeability (C2P), human intestinal absorption (HIV), and P-glycoprotein inhibitor (P-gpI) were used to predict the absorption level of galactopyranosides (Table 2). The C2P of compounds 5 and 6 were found to be higher than that of other galactopyranosides. The addition of ester groups increased the HIA of all compounds, with compounds 2-6 having excellent %HIA, even better than that of fluconazole. Overall, the esters were predicted to be easily absorbed by HIA.

Blood-brain barrier (BBB) membrane permeability and central nervous system (CNS) permeability were used to characterize the distribution of galactopyranosides. The BBB values, as presented in Table 2, indicated that the SEs could moderately cross BBB. However, the compounds, comparable to the fluconazole, were able to penetrate through CNS (Table 2). While compounds 1-3 were found to be CYP3A4 substrate, the rest of the compounds (*i.e.,* 4-6) were found to be non-substrate. Total renal clearance of all the SEs was found to be higher than that of fluconazole.

The acute toxicity of compounds 1-6 was predicted and expressed as hERG (the human Ether-à-go-go-Related Gene) inhibition and oral rat LD_{50} values. Compounds that inhibit or block the hERG potassium channels can potentially cause life-threatening arrhythmias [49]. In this study, all galactopyranosides were non-inhibitor of hERG and thus can be considered safe. These molecules had good LD_{50} values compared to those of fluconazole. Overall, the predicted toxicity parameters of the compounds were in good agreement with those of fluconazole.

DFT-optimized Calculations of Different Properties

A DFT-based method was used to calculate the thermodynamic properties of the compounds and predict the stability and other inherent properties of molecules. The results of the DFT calculations were used to estimate the thermodynamic stability of galactopyranosides 1-6 and

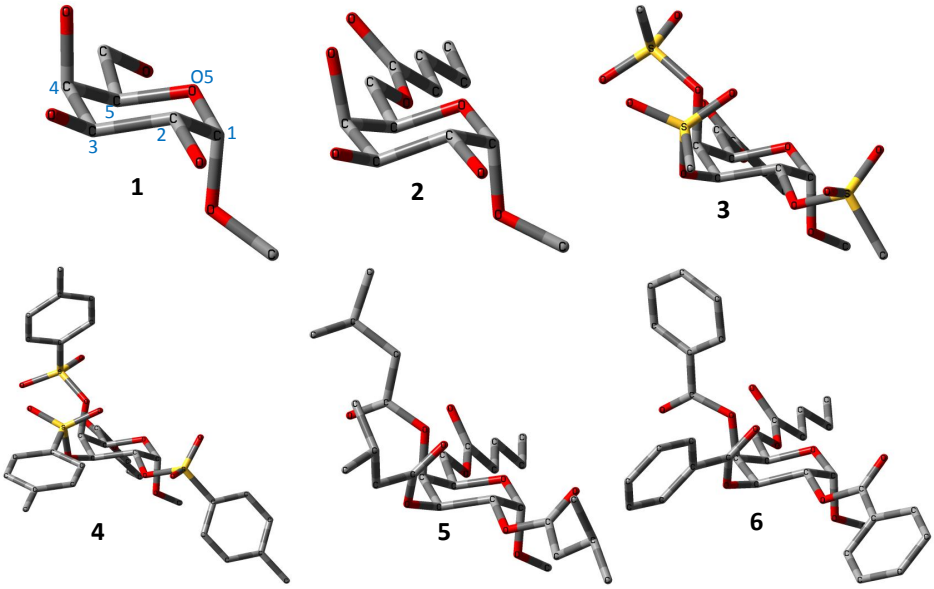

Fig. 1. DFT (B3LYP/6-31G,d,p)-optimized structures of galactopyranosides 1-6.

Table 3. RB3LYP Energy (Hartree), Internal Energy (IE) (Hartree), Enthalpy (Hartree), Gibbs Free Energy (GFE) (Hartree), Entropy (cal mol^{-1} K^{-1}), and Dipole Moment (DM, Debye) of 1-6

Drug	MF	Energy	IE	Enthalpy	GFE	Entropy	DM (μ)
1	$C_7H_{14}O_6$	-726.7054	-726.4665	-726.4656	-726.5208	116.188	1.2769
2	$C_{12}H_{22}O_7$	-997.3825	-997.0139	-997.0130	-997.0887	159.420	1.1957
3	$C_{15}H_{28}O_{13}S_3$	-2761.2812	-2760.7857	-2760.7848	-2760.8940	229.948	8.2289
4	$C_{33}H_{40}O_{13}S3$	-3453.9463	-3453.1917	-3453.1907	-3453.3395	313.074	7.9937
5	$C_{27}H_{46}O_{10}$	-1808.9515	-1808.1902	-1808.1892	-1808.3207	276.578	3.5163
6	$C_{33}H_{34}O_{10}$	-2030.3304	-2029.6673	-2029.6663	-2029.7910	262.325	4.0331

calculate MO and MEP energies.

Thermodynamic properties. The structures of MDG 1 and its different esters (2-6) optimized by DFT (B3LYP/6-31G(d,p) basis set at 298.15 K and 1.0 atm are shown in Fig. 1 (H atoms are not shown for clarity). All the molecules were found to have almost similar conformations and the same C1 symmetry.

The thermodynamic properties of these compounds, such as their optimized energy, internal energy, enthalpy (ΔH), Gibbs free energy (G), entropy and dipole moment (μ), were calculated at 298.15 K and 1.0 atm, and the results are presented in Table 3.

It is known that the lower the energy of a molecule is, the more tightly its electron is bound to the nucleus and, hence, the more stable the molecule will be. In this study, with an increase in the number of acyl group(s) attached to galactopyranoside 1, the level of RB3LYP energy gradually decreased in galactopyranosides 2-6. Sulfonyl esters 3 and 4 had the lowest energy, indicating that they had the highest stability. Internal energy and enthalpy of esters 2-6 were

Table 4. Bond and Dihedral Angles of MDG 1-6

Molecule	Bond angle in degree					
	O5-C1-C2	C1-C2-C3	C2-C3-C4	C3-C4-C5	C4-C5-O5	C5-O5-C1
1	107.75	110.18	110.88	110.88	111.88	114.55
2	108.95	109.85	110.41	109.84	112.03	114.51
3	109.89	110.16	111.60	107.35	110.41	114.52
4	109.53	106.07	109.79	108.70	110.45	113.84
5	109.84	108.77	110.77	108.76	110.92	114.34
6	109.44	108.80	111.41	108.96	111.20	114.16

*The values were calculated from their optimized structures.

also lower than those of non-ester galactopyranoside 1. Gibbs free energy (G), which includes both enthalpy and entropy, shows the spontaneity of a reaction at $G < 0$. With an increase in the size and number of ester groups, G values decreased in groups 2-6 more than in group 1 (Table 3), indicating the spontaneous binding of esters 2-6 to other substrates, such as enzymes, in their biological activities. Dipole moment (μ) is the measure of net molecular polarity and reflects binding affinity. The mesyl ester 3 had the highest μ (8.2289 Debye), followed by the tosyl ester 4 (7.9937 Debye). In general, the attachment of acyl group(s) was found to increase the stability, polarity, spontaneous binding, and interaction of galctopyranoside esters 2-6 with other substrates.

Conformations of galactopyranosides 1-6. It can be seen from Fig. 1 that these Gal compounds existed in the normal $^4C_1$ conformation. However, to confirm this finding, the bond angles of the pyranose ring of ester compounds 2-6 were compared with those of non-ester 1 (Table 4). Gal 1 is well-known to be present in the $^4C_1$ conformation. Compared to the introduction of the original compound 1, the introduction of ester groups at different ring positions (C-2, C-3 and C-4) slightly changed the ring bond angles (Table 4). In a previous study, we found that a large difference of bond angles occurred during the deviation from the normal chair conformation of monosaccharide molecules [50]. In the present study, the very small bond angle changes which occurred due to the attachment of acyl groups showed that the MDG esters 2-6 had an almost normal $^4C_1$ chair conformation.

MO Analysis. MO theory is the most important quantum mechanical theory for describing and approximating molecular bonding. In this study, MOs, especially HOMO (highest occupied molecular orbital) and LUMO (lowest unoccupied molecular orbital) energies, were calculated for all the compounds based on their DFT-optimized structures. Then, the HOMO-LUMO energy gap ($\Delta\varepsilon$) was used for the calculation of molecular hardness (η; $\eta = \Delta\varepsilon/2$) and softness ($S$, $S = 1/\eta$) of galactopyranosides 1-6. When the HOMO and LUMO orbital energies are closest to any molecular orbitals with different energy levels, the HOMO-LUMO gap is the most likely area where excitation energies may occur. HOMO-LUMO energy gap ($\Delta\varepsilon$) and other relevant properties of all galactopyranosides (1-6) are presented in Table 5.

As is evident from Table 4, the HOMO-LUMO energy gap ($\Delta\varepsilon$) values of mesyl ester 3 (Fig. 2a) and isovaleryl ester 5 (Fig. 2b) are higher than that of the non-ester MDG (1). Hence, mesyl ester 3 and isovaleryl ester 5 are less reactive and more stable. However, the HOMO-LUMO energy gap ($\Delta\varepsilon$) values of tosyl ester 4 and benzoyl ester 6 are lower than 1, indicating that esters 4 and 6 can be relatively more easily photochemically excited than esters 1, 3 and 5. Accordingly, the molecular hardness of esters 1, 3, and 5 seems to be higher than that of esters 4 and 6.

MEP Analysis. The MEP is the potential energy of a proton at a particular location near a molecule. While the negative electrostatic potential corresponds to an attraction of the proton by the concentrated electron density in the molecule, generally colored in shades of red, and is a

Table 5. HOMO and LUMO Energies (eV), Energy Gap, and Molecular Hardness and Softness of Galactopyranosides 1-6

Drug	εHOMO	LUMO	Gap ($\Delta\varepsilon$)	Hardness (η)	Softness (S)
1	-7.478	-0.526	6.958	3.479	0.287
2	-7.342	-0.524	6.818	3.409	0.293
3	-7.725	-0.592	7.133	3.567	0.280
4	-6.876	-1.206	5.670	2.835	0.353
5	-7.332	+0.113	7.445	3.723	0.269
6	-6.910	-1.333	5.577	2.789	0.359

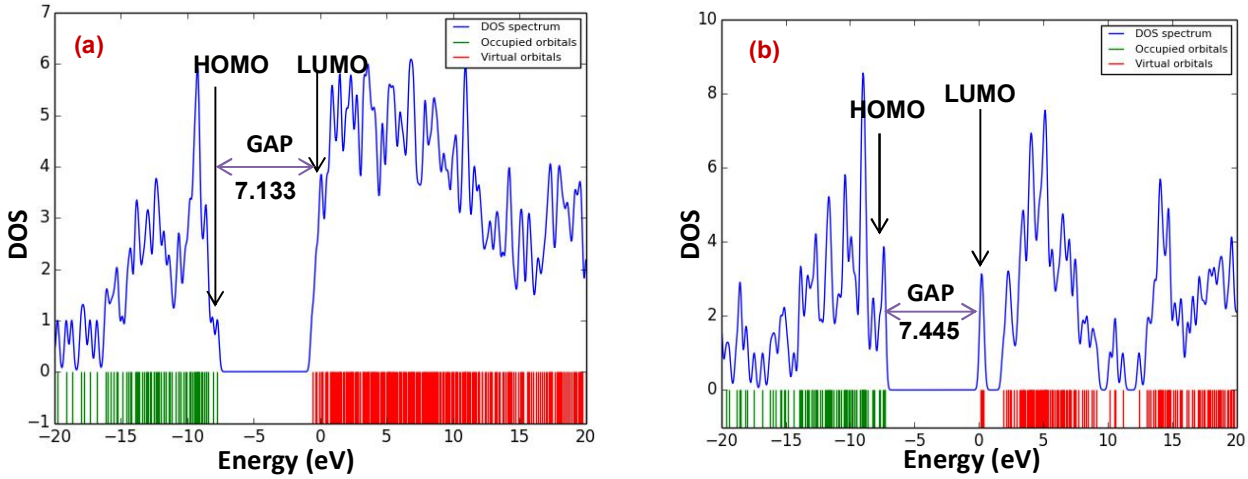

Fig. 2. DOS plot of esters (a) 3 and (b) 5 for the HOMO-LUMO gap.

favorable site for the electrophilic attack, the positive electrostatic potential corresponds to the repulsion of the proton by the atomic nuclei in regions where low electron density exists, usually colored in shades of blue, and is a favorable site for nucleophilic attack. The more the red-blue difference is, the more polar the molecule is. If the surface is largely white or colored with lighter shades, the molecule is mostly nonpolar. The MEP surfaces of galactopyranosides 1-6 are shown in Fig. 3.

The MEP analysis (Fig. 3) showed that the incorporation of ester groups into MDG (1, -0.1560 eV) gradually increased its negative red color (-0.2026 to -0.2236 eV).

Therefore, it can be stated that ester groups increased the maximum rate of the electrophilic attack in the molecule. In the case of sulfonyl esters 3 (+0.3139 eV) and 4 (+0.3270 eV), their positive electrostatic potential, illustrated by shades of blue, increased more than that of sulfonyl ester 1 (+0.1847 eV). On the contrary, the positive electrostatic potential of sulfonyl esters 2, 5 and 6 decreased. As a result, the red-blue differences are more pronounced for esters 3 and 4, confirming their high dipole moment (μ) (Table 3).

CONCLUSIONS

Several galactopyranoside-based novel SEs, starting

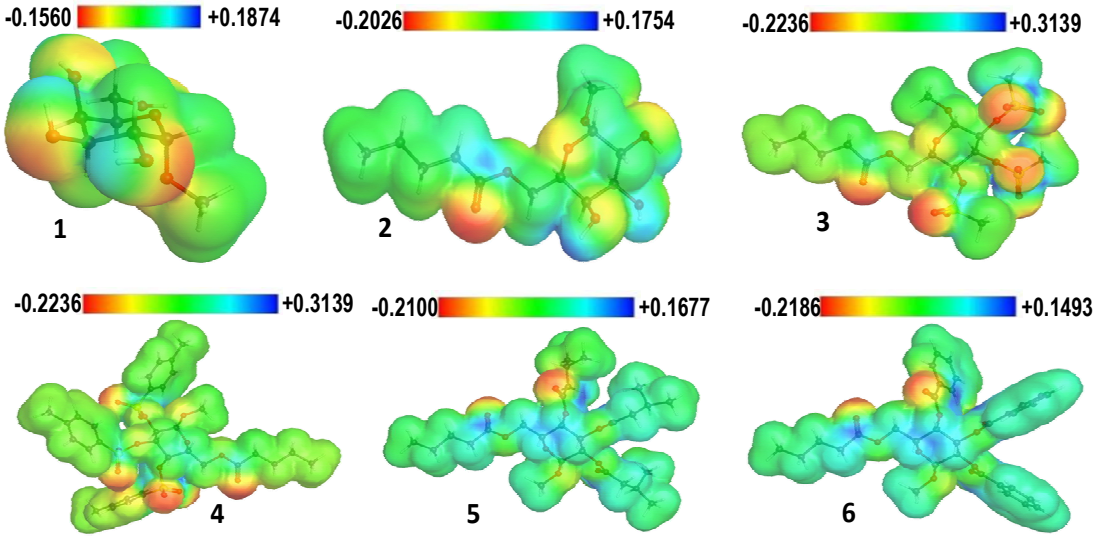

Fig. 3. MEP (eV) of compounds 1-6.

from methyl α-d-galactopyranoside (1), were synthesized and characterized successfully. The biological activities of all the synthesized compounds (1-6) were predicted by PASS online software. The results showed that the addition of the isopentanoyl group, as in 5, increased the antibacterial and antifungal properties of all compounds, even more significantly than did the addition of the 6-*O*-pentanoate 2. Also, the alkyl ester compounds were found to have higher antimicrobial potential than the sulfonyl ester compounds. ADMET prediction showed that the SEs had a high safety profile and thus could be considered as promising drug candidates. More importantly, this study indicated that the addition of ester groups improved various thermodynamic properties, such as stability, polarity, spontaneous binding, and interaction with other substrates, of the Gal esters (2-6). Also, the related MO and MEP properties of different ester groups (1-6) were discussed above.

ACKNOWLEDGEMENTS

We gratefully acknowledge the financial support from the Ministry of Education, Bangladesh, and BANBEIS (grant no. PS 201660, 2016-17).

Conflict of Interest

The authors declare no conflict of interest. All authors have approved the final version of the manuscript.

REFERENCES

[1] Masuyer, G.; Jabeen, T.; Oberg, C. T.; Leffler, H.; Nilsson, U. J.; Acharya, K. R., Inhibition mechanism of human galectin-7 by a novel galactose-benzylphosphate inhibitor. *FEBS J.* **2012**, *279*, 193-202, DOI: 10.1111/j.1742-4658.2011.08414.

[2] Dhavale, D. D.; Matin, M. M., Selective sulfonylation of 4-C-hyroxymethyl-β-L-threo-pento-1,4-furanose: Synthesis of bicyclic diazasugars. *Tetrahedron* **2004**, *60*, 4275-4281, DOI: 10.1016/j.tet.2004.03.034.

[3] Suzuki, Y.; Toda, Y.; Tamatani, T.; Watanabe, T.; Suzuki, T.; Nakao, T.; Murase, K.; Kiso, M.; Hasegawa, A.; Tadanoaritomi, K.; Ishizuka, I.; Miyasaka, M., Sulfated glycolipids are ligands for a lymphocyte homing receptor, L-selectin (LECAM-1), Binding epitope in sulfated sugar chain. *Biochem. Biophys. Res. Commun.* **1993**, *190*, 426-434, DOI: 10.1006/bbrc.1993.1065.

[4] Lv, Y.; Yu, G., Galactose: Structure and Function in Biology and Medicine. Nova Science Publishers (NY, USA), **2014**, pp. 1-24. ISBN: 978-1-63117-928-0.

[5] Hussain, M. R. M.; Hassan, M.; Shaik, N. A.; Zeeshan Iqbal, Z., The role of Galactose in human health and disease. *Cent. Eur. J. Med.* **2012**, *7*, 409-419, DOI: 10.2478/s11536-012-0022-z.

[6] Qi, X.; Tester, R. F., Fructose, galactose and glucose - In health and disease. *Clinical Nutrition ESPEN* **2019**, *33*, 18-28, DOI: 10.1016/j.clnesp.2019.07.004.

[7] Dhavale, D. D.; Matin, M. M.; Sharma, T.; Sabharwal, S. G., N-Hydroxyethyl-piperidine and -pyrrolidine homoazasugars: Preparation and evaluation of glycosidase inhibitory activity. *Bioorg. Med. Chem.* **2003**, *11*, 3295-3305, DOI: 10.1016/S0968-0896(03)00231-1.

[8] Huang, L. H.; Yan, Q. J.; Kopparapu, N. K.; Jiang, Z. Q.; Sun, Y., Astragalus membranaceus lectin (AML) induces caspase-dependent apoptosis in human leukemia cells. *Cell Prolif.* **2012**, *45*, 15-21, DOI: 10.1111/j.1365-2184.2011.00800.x.

[9] Fontaine, T.; Delangle, A.; Simenel, C.; Coddeville, B.; van Vliet, S. J.; van Kooyk, Y.; Bozza, S.; Moretti, S.; Schwarz, F.; Trichot, C.; Aebi, M.; Delepierre, M.; Elbim, C.; Romani, L.; Latgé, J. P., Galactosaminogalactan, a new immunosuppressive polysaccharide of Aspergillus fumigatus. *PLoS Pathog.* **2011**, *7*, e1002372, DOI: 10.1371/journal.ppat.1002372.

[10] Gomes, M. M.; Suzuki, H.; Brooks, M. T.; Tomana, M.; Moldoveanu, Z.; Mestecky, J.; Julian, B. A.; Novak, J.; Herr, A. B., Recognition of galactose-defcient O-glycans in the hinge region of IgA1 by N-acetylgalactosaminespecifc snail lectins: a comparative binding study. *Biochemistry* **2010**, *49*, 5671-5682, DOI: 10.1021/bi9019498.

[11] Kaleem, A.; Khurshid, A.; Ahmad, I.; Walker-Nasir, E.; Khan, S.; Choudhary, M. I.; Shakoori, A. R.; Nasir-Ud-Din, terminal galactose as cancer recognition marker: Computing analysis with implications of vicinal sugars, linkage and anomery. *Pakistan J. Zool.* **2008**, *40*, 135-143. DOI: ?

[12] Loveless, R. W.; Yuen, C. T.; Tsuiji, H.; Irimura, T.; Feizi, T., Monoclonal antibody 91.9H raised against sulfated mucins is specific for the 3'-sulfated Lewis a tetrasaccharide sequence. *Glycobiology* **1998**, *8*, 1237-1242, DOI: 10.1093/glycob/8.12.1237.

[13] Galili, U., Evolution and pathophysiology of the human natural anti-alpha-galactosyl IgG (anti-Gal) antibody. *Springer Semin Immunopathol.* **1993**, *15*, 155-171, DOI: 10.1007/BF00201098.

[14] Matin, M. M., Synthesis of some silyl protected 1,4-galactonolactone derivatives. *J. Appl. Sci. Res.* **2006**, *2*, 753-756.

[15] Varki, A., Evolutionary forces shaping the Golgi glycosylation machinery: Why cell surface glycans are universal to living cells. *Cold Spring Harb Perspect Biol.* **2011**, DOI: 10.1101/cshperspect.a005462.

[16] Shah, S. M.; Goel, P. N.; Jain, A. S.; Pathak, P. O.; Padhye, S. G.; *et al.*, Liposomes for targeting hepatocellular carcinoma: use of conjugated arabinogalactan as targeting ligand. *Int. J. Pharm.* **2014**, *477*, 128-139, DOI: 10.1016/j.ijpharm.2014.10.014.

[17] Liu, M. J.; Ding Qu, D.; Chen, Y.; Liu, C. Y.; Liu, Y. P.; Ding, X. F., Preparation of novel butyryl galactose ester-modified coix component microemulsions and evaluation on hepatoma-targeting *in vitro* and *in vivo*. *Drug Delivery* **2016**, *23*, 3444-3451, DOI: 10.1080/10717544.2016.1189984.

[18] Chang, S. W.; Shaw, J. F., Biocatalysis for the production of carbohydrate esters, *New Biotechnol.* **2009**, *26*, 109-116, DOI: 10.1016/j.nbt.2009.07.003.

[19] Matin, M. M.; Bhuiyan, M. M. H.; Kabir, E.; Sanaullah, A. F. M.; Rahman, M. A.; Hossain, M. E.; Uzzaman, M., Synthesis, characterization, ADMET, PASS predication, and antimicrobial study of 6-O-lauroyl mannopyranosides. *J. Mol. Struct.* **2019**, *1195*, 189-197, DOI: 10.1016/j.molstruc.2019.05.102.

[20] Matin, M. M.; Chakraborty, P.; Alam, M. S.; Islam, M. M.; Hanee, U., Novel mannopyranoside esters as sterol 14α-demethylase inhibitors: Synthesis, PASS predication, molecular docking, and pharmacokinetic studies. *Carbohydr. Res.* **2020**, *496*, 108130, DOI: 10.1016/j.carres.2020.108130.

[21] Matin, M. M.; Bhuiyan, M. M. H.; Azad, A. K. M. S.; Akther, N., Design and synthesis of benzyl-4-O-

lauroyl-α-L-rhamnopyranoside derivatives as antimicrobial agents. *Current Chem. Lett.* **2017**, *6*, 31-40, DOI: 10.5267/j.ccl.2016.10.001.

[22] Matin, M. M.; Uzzaman, M.; Chowdhury, S. A.; Bhuiyan, M. M. H., *In vitro* antimicrobial, physicochemical, pharmacokinetics, and molecular docking studies of benzoyl uridine esters against SARS-CoV-2 main protease. *J. Biomol. Struct. Dyn.* **2020**, DOI: 10.1080/07391102.2020.1850358; PMID: 33297848; PMCID: PMC7738211.

[23] Yousefi, S.; Bayata, S.; Rahmana, M. B. A.; Ibrahima, Z.; Abdulmalek, E., Synthesis and *in vitro* bioactivity evaluation of new galactose and fructose ester derivatives of 5-aminosalicylic acid. *Chem. Biodiversity* **2017**, *14*, e1600362, DOI: 10.1002/cbdv.201600362.

[24] Yadav, R.; Mahatma, O. P., Ester prodrug of 5-Aminosalicylic acid for colon specific drug delivery: Synthesis, kinetics, hydrolysis and stabilities studies. *J. Pharm. Sci. Res.* **2011**, *3*, 966-972.

[25] Miljkovic, M., Relative Reactivity of Hydroxyl Groups in Monosaccharides. In: Carbohydrates. Springer (New York), 2010.

[26] Lee, D.; Taylor, M. S., Catalyst-controlled regioselective reactions of carbohydrate derivatives. *Synthesis* **2012**, *44*, 3421-3431. DOI: 10.1055/s-0032-1317483.

[27] Matin, M. M.; Iqbal, M. Z., Methyl 4-O-(2-chlorobenzoyl)-α-L-rhamnopyranosides: Synthesis, characterization, and thermodynamic studies. *Orbital: Electron. J. Chem.* **2021**, *13*, 19-27. DOI: 10.17807/orbital.v13i1.1532.

[28] Dimakos, V.; Taylor, M. S., Site-selective functionalization of hydroxyl groups in carbohydrate derivatives. *Chem. Rev.* **2018**, *118*, 11457-11517, DOI: 10.1021/acs.chemrev.8b00442.

[29] Matin, M. M.; Bhattacharjee, S. C.; Chakraborty, P.; Alam, M. S., Synthesis, PASS predication, *in vitro* antimicrobial evaluation and pharmacokinetic study of novel n-octyl glucopyranoside esters. *Carbohydr. Res.* **2019**, *485*, 107812, DOI: 10.1016/j.carres.2019.107812.

[30] Matin, M. M.; Hasan, M. S.; Uzzaman, M.; Bhuiyan, M. M. H.; Kibria, S. M.; Hossain, M. E.; Roshid, M. H. O., Synthesis, spectroscopic characterization, molecular docking, and ADMET studies of mannopyranoside esters as antimicrobial agents. *J. Mol. Struct.* **2020**, *1222*, 128821, DOI: 10.1016/j.molstruc.2020.128821.

[31] Lawandi, J.; Rocheleau, S.; Moitessier, N., Regioselective acylation, alkylation, silylation and glycosylation of monosaccharides. *Tetrahedron* **2016**, *72*, 6283-6319, DOI: 10.1016/j.tet.2016.08.019.

[32] Matin, M. M.; Bhuiyan, M. M. H.; Azad, A. K.M. S.; Rashid, M. H. O., Synthesis of 6-O-stearoyl-1,2-O-isopropylidene-α-D-gluco-furanose derivatives for antimicrobial evaluation. *J. Physical Sci.* **2015**, *26*, 1-12.

[33] Matin, M. M., Synthesis of D-glucose derived oxetane: 1,2-O-Isopropylidene-4-(S)-3-O,4-C-methylene-5-O-methanesulfonyl-β-L-threo-pento-1,4-furanose. *J. Appl. Sci. Res.* **2008**, *4*, 1478-1482.

[34] Matin, M. M.; Bhuiyan, M. H.; Hossain, M. M.; Roshid, M. H. O., Comparative antibacterial activities of some monosaccharide and disaccharide benzoates. *Orbital: Electron. J. Chem.* **2015**, *7*, 160-167, DOI: 10.17807/orbital.v7i2.699.

[35] Matin, M. M.; Islam, N.; Siddika, A.; Bhattacharjee, S. C., Regioselective synthesis of some rhamnopyranoside esters for PASS predication, and ADMET studies. *J. Turkish Chem. Soc. Sect. A: Chem.* **2021**, *8*, 363-374, DOI: 10.18596/jotcsa.829658.

[36] Medgyes, G.; Jerkovich, G.; Kuszmann, J.; Fügedi, P., Synthesis of sorbistin analogues. Carbohydr. Res. **1989**, 186, 225-239, DOI: 10.1016/0008-6215(89)84037-6.

[37] Matin, M. M.; Ibrahim, M., Synthesis of some methyl 4-O-octanoyl-α-L-rhamnopyranoside derivatives. *J. Appli. Sci. Res.* **2010**, *6*, 1527-1532.

[38] Matin, M. M., Synthesis and antimicrobial study of some methyl 4-O-palmitoyl-α-L-rhamnopyranoside derivatives. *Orbital: Electron. J. Chem.* **2014**, *6*, 20-28, DOI: 10.17807/orbital.v6i1.553.

[39] Xu, Y.; Masuko, S.; Takieddin, M.; Xu, H.; Liu, R.; Jing, J.; Mousa, S. A.; Linhardt, R. J.; Liu, J., Chemoenzymatic synthesis of homogeneous ultralow molecular weight heparins. *Science* **2011**, *334*, 498-

501, DOI:10.1126/science.1207478.

[40] Ortiz, Á. D.; Prieto, P.; de la Hoz, A., A critical overview on the effect of microwave irradiation in organic synthesis. *The Chem. Record* **2019**, *19*, 85-97, DOI: 10.1002/tcr.201800059.

[41] Compound 2, ^{1}H NMR (400 MHz, $CDCl_3$): δH 4.92 (d, J = 3.2 Hz, 1H, H-1), 4.36 (dd, J = 11.6 and 4.4 Hz, 1H, H-6), 4.27 (dd, J = 11.6 and 6.4 Hz, 1H, H-6′), 3.78-3.98 (m, 4H, H-2, H-3, H-4 and H-5), 3.42 (s, 3H, OCH_3), 3.21-3.38 (br s, 3H, 3×OH), 2.35 [t, J = 7.6 Hz, 2H, $CH_3(CH_2)_2CH_2CO$], 1.58-1.69 (m, 2H, $CH_3CH_2CH_2CH_2CO$), 1.27-1.43 [m, 2H, $CH_3CH_2(CH_2)2CO$], 0.92 [t, 3H, J = 7.2 Hz, $CH_3(CH_2)_3CO$].

[42] Wu, W.; Cheng, Y.; Guo, B. -H.; Wu, Q., Pharmacokinetics of liver-targeted docetaxel liposomes modified with 6-O-acyl-D-galactose esters in rabbits. *Biomed. Rep.* **2014**, *2*, 545-548, DIO: 10.3892/br.2014.285.

[43] Matin, M. M.; Nath, A. R.; Saad, O.; Bhuiyan, M. M. H.; Kadir, F. A.; Abd Hamid, S. B.; Alhadi, A. A.; Ali, M. E.; Yehye, W. A., Synthesis, PASS-predication and *in vitro* antimicrobial activity of benzyl-4-O-benzoyl-α-L-rhamnopyranoside derivatives. *Int. J. Mol. Sci.* **2016**, *17*, 1412, DOI: 10.3390/ijms17091412.

[44] Filimonov, D. A.; Lagunin, A. A.; Gloriozova, T. A.; Rudik, A. V.; Druzhilovskii, D. S.; Pogodin, P. V.; Poroikov, V. V., Prediction of the biological activity spectra of organic compounds using the PASS online web resource. *Chem. Hetero. Comp.* **2014**, *50*, 444-457, DOI: 10.1007/s10593-014-1496-1.

[45] Pires, D. E. V.; Blundell, T. L.; Ascher, D. B., pkCSM: Predicting small-molecule pharmacokinetic properties using graph-based signatures. *J. Med. Chem.* **2015**, *58*, 4066. DOI: 10.1021/acs.jmedchem.5b00104.

[46] Matin, M. M.; Chakraborty, P., Synthesis, spectral and DFT characterization, PASS predication, antimicrobial, and ADMET studies of some novel mannopyranoside esters. *J. Appl. Sci. Process Eng.* **2020**, *7*, 572-586, DOI: 10.33736/jaspe.2603.2020.

[47] Frisch, M. J.; Trucks, G. W.; Schlegel, H. B.; Scuseria, G. E.; Robb, M. A.; Cheeseman, J. R.; Scalmani, G.; Barone, V.; Petersson, G. A.; Nakatsuji, H., Gaussian 09, Gaussian Inc. (Wallingford CT), **2013**.

[48] Dong, J.; Wang, N. -N.; Yao, Z. -J.; Zhang, L.; Cheng, Y.; Ouyang, D.; Ai-Ping Lu, A. -P.; Cao, D. -S., ADMETlab: A platform for systematic ADMET evaluation based on a comprehensively collected ADMET database. *J. Cheminform.* **2018**, *10*, 29, DOI: 10.1186/s13321-018-0283-x.

[49] Priest, B.; Bell, I. M.; Garcia, M., Role of hERG potassium channel assays in drug development. *Channels* **2008**, *2*, 87-93, DOI: 10.4161/chan.2.2.6004.

[50] Islam, F.; Rahman, M. R.; Matin, M. M., The effects of protecting and acyl groups on the conformation of benzyl α-L-rhamnopyranosides: An in silico study. *Turkish Comp. Theo. Chem.* **2021**, *5*, 39-50, DOI: 10.33435/tcandtc.914768.